

Quantum spin Hall effect in a disordered hexagonal $\text{Si}_x\text{Ge}_{1-x}$ alloy

J. E. Padilha,^{1,*} L. Seixas,^{1,†} Renato B. Pontes,^{2,‡} Antônio J. R. da Silva,^{1,3,§} and A. Fazzio^{1,||}

¹*Instituto de Física, Universidade de São Paulo, CP 66318, 05315-970, São Paulo, SP, Brazil*

²*Instituto de Física, Universidade Federal de Goiás, CP 131, 74001-970, Goiânia, GO, Brazil*

³*Laboratório Nacional de Luz Síncrotron - LNLS, Campinas, SP, Brazil*

(Received 12 February 2013; revised manuscript received 1 November 2013; published 15 November 2013)

We show that the $\text{Si}_x\text{Ge}_{1-x}$ random alloys in the honeycomb monolayer structure are nontrivial topological insulators with the same topological classification $Z_2 = 1$ as pristine silicene and germanene. The application of an external electric field decreases the band gap up to its closure at a critical value of the field, $|E_c|$. For absolute values of the field larger than $|E_c|$ the band gap increases again, and the systems are now trivial insulators. Thus, similarly to what happens for zinc-blend $\text{Si}_x\text{Ge}_{1-x}$ alloys, these materials will bring new possibilities in the design of devices, such as band gap and mobility engineering, with the added feature that they will exhibit a quantum spin Hall effect due to the gap generated by the spin-orbit coupling.

DOI: [10.1103/PhysRevB.88.201106](https://doi.org/10.1103/PhysRevB.88.201106)

PACS number(s): 71.70.Ej, 63.50.Gh, 71.15.Nc, 73.22.—f

Considerable progress has been made to have a complete understanding of the electronic properties of graphene. It has attracted attention of the scientific community due to its potential to be used in nanodevices.¹ Graphene²⁻⁴ is a truly two-dimensional (2D) planar material, with a honeycomb crystal lattice. Their valence and conduction bands, in the absence of spin-orbit coupling (SOC), cross at the Fermi level in a conical shape, with a linear energy-momentum dispersion relation at two k points (K and K') of the Brillouin zone, the Dirac points. Kane and Mele⁵ have shown that a single layer of graphene could exhibit quantum spin Hall effect (QSHE) due to the SOC opening a small gap. However, the size of the gap would not allow the observation of the QSHE at realistic temperatures.^{6,7}

Recently, a new material, named silicene,⁸⁻¹³ has been synthesized. It shares the same structure with graphene, but with two important differences:¹⁴⁻¹⁸ (i) the honeycomb structure is buckled and (ii) it has a relatively larger SOC and, thus, a larger spin-orbit band gap. As a result, this material could be a possible candidate for the observation of the QSHE as proposed by Kane and Mele.¹⁹⁻²¹

Besides silicene, Liu *et al.*²² have recently shown that germanene as well could display a QSH effect at experimentally accessible temperatures. Moreover, the buckling structure of these hexagonal materials brings out a new feature when compared to graphene, which is the possibility to tune the band gap by the application of an electric field perpendicular to the atomic layer.^{16,18,23} Even more interestingly, for absolute values of the electric field smaller than a critical value $|E_c|$, the system behaves as a $Z_2 = 1$ topological insulator (TI), whereas for absolute values greater than $|E_c|$, the system is an ordinary band insulator. The overall behavior of the band gap, observed for both silicene and germanene, as a function of the external electric field, is a W-shaped function, with the band gap closing at $|E_c|$. The only difference between these materials is the value of $|E_c|$, which is connected to the strength of the SOC, which is larger in germanene than in silicene, resulting also in a larger band gap in the former (28 meV) than in the latter (1.95 meV).

If we consider zinc-blend (ZB) bulk materials, the possibility of mixing Si and Ge to optimize the material properties has been already a reality for many years, since $\text{Si}_x\text{Ge}_{1-x}$ forms a

random alloy which has been used in a variety of devices.^{24,25} Thus, there is also the possibility of employing $\text{Si}_x\text{Ge}_{1-x}$ alloy monolayers with 2D honeycomb geometry in new devices that present quantum spin Hall effect, with the added feature of band gap engineering.

In this Rapid Communication we show that a truly disordered $\text{Si}_x\text{Ge}_{1-x}$ alloy monolayer with 2D honeycomb geometry, for any value of x , is a nontrivial insulator with the same topological classification as silicene and germanene. This statement is based on two results: (i) The band gap never closes as x is increased from $x = 0$ (germanene) to $x = 1$ (silicene). Thus, the adiabatic continuity argument²⁶⁻³¹ guarantees that the disordered SiGe alloy has the same topological classification as silicene and germanene. (ii) The application of an electric field perpendicular to the $\text{Si}_x\text{Ge}_{1-x}$ monolayer leads to a W-shaped behavior for the band gap, as observed in silicene and germanene,¹⁶ indicating that the disordered alloys are $Z_2 = 1$ TIs.

The electronic structure simulations were performed within the density functional theory (DFT) framework^{32,33} as implemented in the OpenMX code.³⁴ For the exchange-correlation functional we used the GGA-PBE approximation.³⁵ The spin-orbit interaction was included via a norm-conserving fully relativistic j -dependent pseudopotential scheme, in the noncollinear DFT formalism.³⁶ All the systems investigated were fully relaxed until the residual forces on the atoms were smaller than 0.001 eV/Å.

In order to simulate the disordered SiGe alloy in a realistically way using supercells, we employ the special quasirandom structure (SQS) model proposed by Wei *et al.*,³⁷ considering up to the third-nearest neighbors of each atom. This method provides a simple way to determine, via first-principles calculations, the local atomic structure and the electronic properties of a random alloy. It was successfully applied to $\text{Si}_x\text{Ge}_{1-x}$ bulk alloys.³⁸ We used supercells containing 98 atoms of Si and Ge randomly distributed in a honeycomb structure. In our simulations we study the following concentrations of the hexagonal $\text{Si}_x\text{Ge}_{1-x}$ alloy: $x = 18.4\%$, $x = 26.5\%$, $x = 50.0\%$, and $x = 73.5\%$, besides the pure $x = 0\%$ and $x = 100\%$ configurations. In Fig. 1(a) we present a schematic view of the geometry of the disordered $\text{Si}_x\text{Ge}_{1-x}$, illustrated for the particular case of $x = 50\%$. It is well known that the lattice

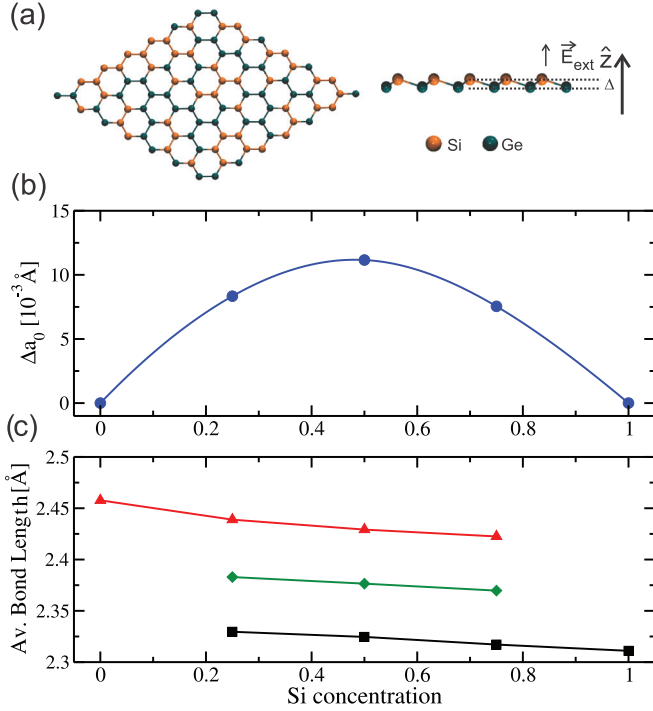


FIG. 1. (Color online) (a) Ball-and-stick model of the disordered $\text{Si}_x\text{Ge}_{1-x}$ 2D hexagonal alloy, for $x = 0.5$, generated with the SQS procedure. We also show in the right panel the buckling height, Δ , and the direction of the applied electric field. (b) Deviation of the alloy equilibrium lattice parameter from linearity, $\Delta a_0(x)$, as defined in the text. (c) Average bond lengths for the Si-Si (squares), Si-Ge (diamonds), and Ge-Ge (triangles) bonds.

parameter of the ZB $\text{Si}_x\text{Ge}_{1-x}$, as a function of x , has a small deviation from linearity.³⁸ To calculate such a deviation for the honeycomb lattice, we first relaxed the supercell and obtained in this way the equilibrium lattice parameter $a_0^{eq}(x)$, for each composition. We then calculated this deviation, $\Delta a_0(x)$, defined as $\Delta a_0(x) = [x a_0^{Si} + (1-x) a_0^{Ge}] - a_0^{eq}(x)$, where a_0^{Si} (a_0^{Ge}) is the lattice parameter for the bulk silicene (germanene). In Fig. 1(b) we present our results for $\Delta a_0(x)$. The results are similar to the zinc-blend $\text{Si}_x\text{Ge}_{1-x}$ alloy, indicating also a negative bowing of the lattice parameter.³⁸ In Fig. 1(c) we plot the average bond lengths as a function of x , for the Si-Si, Si-Ge, and Ge-Ge bonds. As can be seen, the behavior is also very similar to what is obtained for the 3D bulk alloy, indicating that this system is closer to the Pauling rather than the Vegard limit.³⁸ The final geometric parameter we analyzed is the buckling height, Δ , as shown in Fig. 1(a). For pure silicene (germanene) we obtained $\Delta = 0.49 \text{ \AA}$ ($\Delta = 0.71 \text{ \AA}$), and for the alloys we obtained the values 0.66 \AA , 0.61 \AA , and 0.56 \AA , for $x = 26.5\%$, $x = 50.0\%$, and $x = 73.5\%$, respectively.

We also calculate the alloy formation energy, $\Delta E(x)$, defined as $\Delta E(x) = E_{\text{Si}_x\text{Ge}_{1-x}} - [x E_{\text{Si}} + (1-x) E_{\text{Ge}}]$, where $E_{\text{Si}_x\text{Ge}_{1-x}}$, E_{Si} , and E_{Ge} are the total energies per atom for the $\text{Si}_x\text{Ge}_{1-x}$ alloy, silicene, and germanene, respectively. As can be seen from Table I, the values are about four times larger than for the ZB alloy.³⁸ An important parameter is the critical temperature [$T_c(x)$] for the decomposition of the alloy. A simple way to estimate $T_c(x)$ is to equate $\Delta E(x)$ to $T_c(x) \Delta S(x)$, where $\Delta S(x)$ is defined using an equation similar

TABLE I. Alloy formation energy, $\Delta E(x)$, in meV/atom, and the critical decomposition temperature $T_c(x)$, in K. x is the Si composition.

x	$\Delta E(x)$	$T_c(x)$
0.265	13.06	262
0.50	17.58	294
0.735	12.71	255

to the one used for $\Delta E(x)$, with the energy replaced by the entropy. If we only consider the configuration entropy, we have that $\Delta S(x) = -k_B [x \log_{10}(x) + (1-x) \log_{10}(1-x)]$, and from this we can obtain the critical decomposition temperatures, as shown in Table I. As can be seen, even though the temperatures are higher than for the ZB alloy, they are in a range such that the disordered alloy will be stable against decomposition, specially if one considers the growth temperatures.

In Fig. 2 we show the geometries and the calculated electronic band structures³⁹⁻⁴¹ of the $\text{Si}_x\text{Ge}_{1-x}$ alloys for $x = 26.5\%$, $x = 50\%$, and $x = 73.5\%$. The band structures for all concentrations are similar to the bands of pristine silicene and germanene. The only difference is the band gap⁴³ at the K point, (Δ_K), which shows a steady decrease from pristine germanene ($\Delta_K^{Ge} = 25.5 \text{ meV}$) to pristine silicene ($\Delta_K^{Si} = 1.95 \text{ meV}$), as x is varied from $x = 0$ to $x = 1$ [see Fig. 3(a)]. This is shown in detail in Fig. 3(b), where we present the band structures⁴¹ around the K point as a function of x . In Fig. 3(a) we also present, besides the band gap, the bowing $\Delta g(x) = [x \Delta_K^{Si} + (1-x) \Delta_K^{Ge}] - \Delta_K(x)$. As can be seen, the band gap for the alloy presents a small negative bowing.⁴⁴

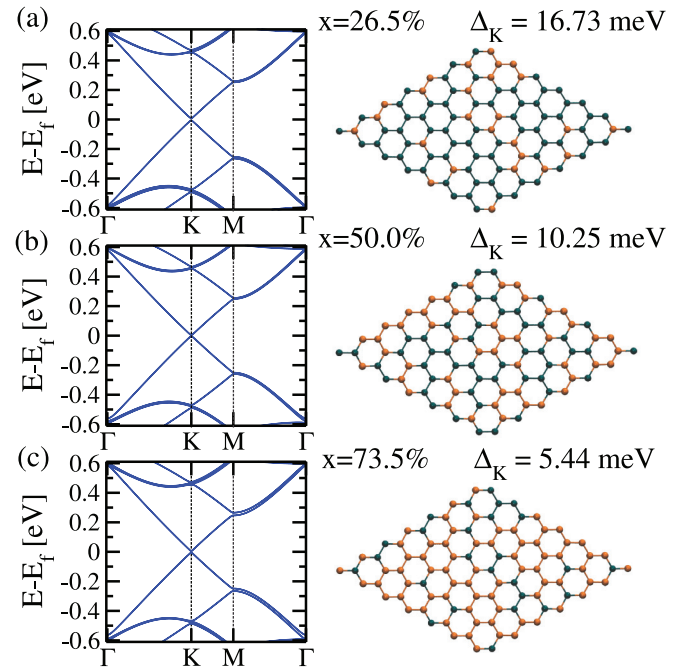


FIG. 2. (Color online) Calculated electronic band structure and geometry of the hexagonal $\text{Si}_x\text{Ge}_{1-x}$ random alloy for (a) $x = 26.5\%$, (b) $x = 50\%$, and (c) $x = 73.5\%$.

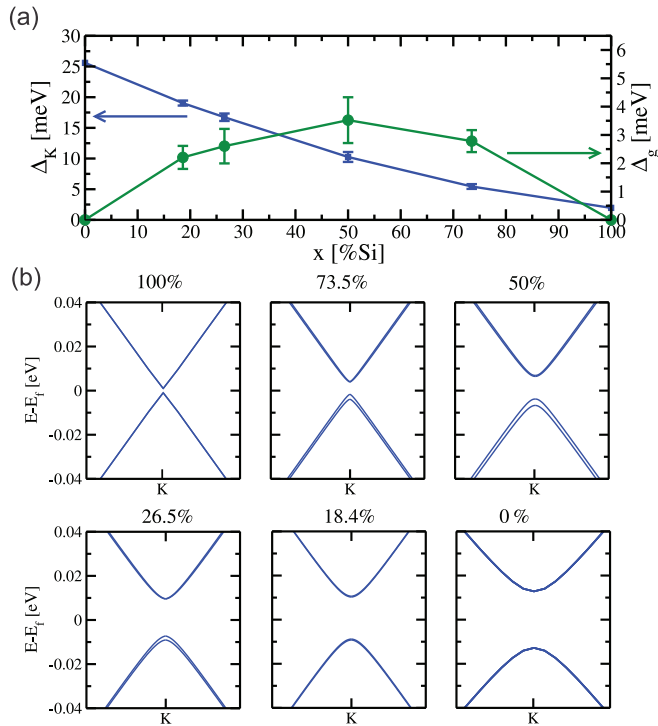


FIG. 3. (Color online) (a) Band gap, Δ_K , and bowing, $\Delta g(x)$, at the K point, as function of the concentration, x , of silicon atoms. The error bars were obtained by performing 30 SQS realizations for each concentration (Ref. 41). (b) Band structure (Ref. 41) around the K point as a function of x . We also present results for $x = 18.4\%$, besides $x = 0\%$, $x = 26.5\%$, $x = 50.0\%$, $x = 73.5\%$, and $x = 100\%$.

We have thus shown that, going from germanene to silicene, which are both $Z_2 = 1$ TIs, passing through the disordered alloys, the band gap never closes. According to the adiabatic continuity argument for the band transformation, which has been used to identify 2D and 3D TIs,^{26–31} if the Hamiltonian of a system is adiabatically transformed into another, the topological classification of the two systems can only change if the band gap closes. Thus, if the band structure of a set of systems can be smoothly changed without closing the gap, all these systems must share the same topological classification. For the $\text{Si}_x\text{Ge}_{1-x}$ alloy, for example, the adiabatic transformation of the band structure can be realized by changing the concentration x . Therefore, we claim that all the $\text{Si}_x\text{Ge}_{1-x}$ disordered alloys fall into the same topological class of pristine silicene and germanene, which is a $Z_2 = 1$ TI. This result is far from trivial. For example, an ordered $\text{Si}_{0.5}\text{Ge}_{0.5}$ alloy has a gap of 7 meV, but is not a topological insulator, as shown in the Supplemental Material.⁴² Moreover, a non-SQS disordered $\text{Si}_{0.5}\text{Ge}_{0.5}$ alloy can have a zero gap (see Supplemental Material⁴²). Thus, it is not simply any mixing of Si and Ge that will result in a TI.

Silicene and germanene undergo a topological phase transition, from a $Z_2 = 1$ topological insulator to a trivial band insulator, as an externally applied electric field is changed. This is manifested as a W-shaped behavior of the band gap as a function of the electric field.¹⁶ Since the random alloy shares the same topological class as silicene and germanene, they should display a similar behavior. In Fig. 4 we show the

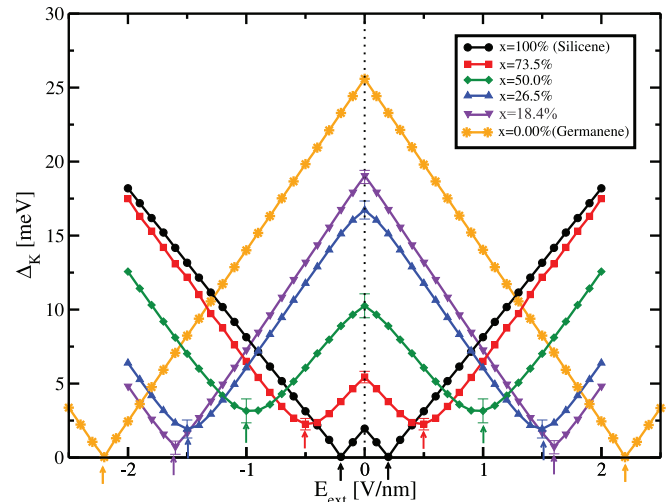


FIG. 4. (Color online) Energy band gap, Δ_K , at the K point, for the $\text{Si}_x\text{Ge}_{1-x}$ alloy, as a function of an applied electric field. The results are shown for five concentrations, x . The arrows below the curves indicate the position of the critical electric field E_c , where there is a quantum topological phase transition from a topological insulator to a band insulator. The error bars shown at these points were obtained by performing 30 SQS realizations for each concentration.

band gap as function of the external electrical field for silicene, germanene, and the $\text{Si}_x\text{Ge}_{1-x}$ alloy.

We can see that, independently of the concentration of silicon, the behavior of the band gap as a function of the electric field is the same. For example, for $x = 50\%$ without an electric field, the system presents a gap of approximately 10.25 meV. When the field is increased to $|E_c| = 1.0$ V/nm, as happens for both silicene and germanene, the band gap tends to close. In fact, the alloy band gaps from Fig. 4 do not go to zero because of finite-size effects. As shown in Fig. 5 for the $\text{Si}_{0.265}\text{Ge}_{0.735}$ alloy, as the size of the supercell increases the band gap decreases, going to zero asymptotically for an infinite system. A similar behavior is observed for other values of x . For absolute values of the electric field larger than $|E_c|$, the energy band gap increases again. This feature is present in all

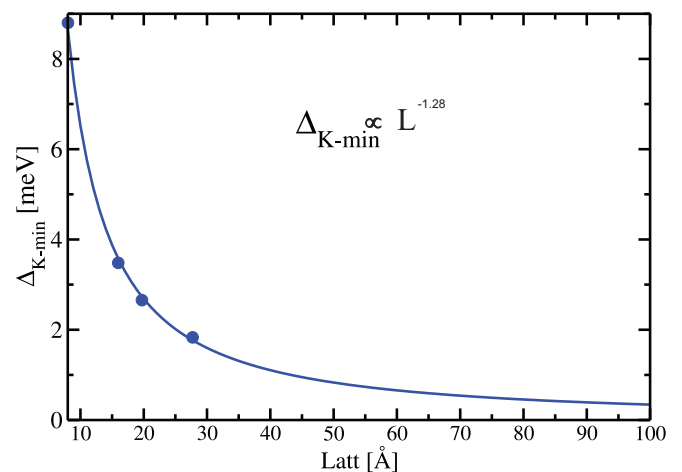


FIG. 5. (Color online) Minimum energy band gap, $\Delta_{K,min}$, at the critical electric field value $|E_c|$, for the $\text{Si}_{0.265}\text{Ge}_{0.735}$ alloy, as a function of the supercell size.

alloys that we have investigated.⁴⁵ Thus, we have shown that random $\text{Si}_x\text{Ge}_{1-x}$ alloys behave exactly like pristine silicene and germanene,¹⁶ being a topological insulator for absolute values of an external electric field smaller than $|E_c|$ and a trivial insulator for values larger than $|E_c|$.

In conclusion, we have shown that truly random $\text{Si}_x\text{Ge}_{1-x}$ alloys are nontrivial topological insulators, with the same topological classification ($Z_2 = 1$) as pristine silicene and germanene. It is important to note that not any mixing of Si and Ge will lead to TIs. Only truly disordered systems seems to present such a behavior. Moreover, only in the limit of very large (infinite) systems is the W-shaped behavior identical to the pristine Si and Ge. This seems to imply that

one needs large systems to recover, in an average way, the homogeneity of the system to guarantee that for any x the disordered $\text{Si}_x\text{Ge}_{1-x}$ is a truly TI. Similarly to the case for ZB $\text{Si}_x\text{Ge}_{1-x}$ alloys, this brings new opportunities to design new devices, where parameters such as band gap and mobility can be tuned by changing the value of x , with the important added feature that they will also present the quantum spin Hall effect. Moreover, the band gap can be further tuned by an externally applied electric field, with the systems keeping their nontrivial topological characteristics up to a critical value $|E_c|$.

The authors thank the Brazilian agencies CAPES, FAPESP, and INCT/CNPq for financial support.

*padilha@if.usp.br

†lseixas@if.usp.br

‡pontes@if.usp.br

§ajrsilva@if.usp.br

¶fazzio@if.usp.br

¹F. Schwierz, *Nat. Nanotechnol.* **5**, 487 (2010).

²K. S. Novoselov, A. K. Geim, S. V. Morozov, D. Jiang, Y. Zhang, S. V. Dubonos, I. V. Grigorieva, and A. A. Firsov, *Science* **306**, 666 (2004).

³A. K. Geim and K. S. Novoselov, *Nat. Mater.* **6**, 183 (2007).

⁴A. H. Castro Neto, F. Guinea, N. M. R. Peres, K. S. Novoselov, and A. K. Geim, *Rev. Mod. Phys.* **81**, 109 (2009).

⁵C. L. Kane and E. J. Mele, *Phys. Rev. Lett.* **95**, 226801 (2005).

⁶H. Min, J. E. Hill, N. A. Sinitsyn, B. R. Sahu, L. Kleinman, and A. H. MacDonald, *Phys. Rev. B* **74**, 165310 (2006).

⁷Y. Yao, F. Ye, X.-L. Qi, S.-C. Zhang, and Z. Fang, *Phys. Rev. B* **75**, 041401 (2007).

⁸B. Aufray, A. Kara, S. Vizzini, H. Oughaddou, C. Leandri, B. Ealet, and G. Le Lay, *Appl. Phys. Lett.* **96**, 183102 (2010).

⁹B. Lalmi, H. Oughaddou, H. Enriquez, A. Kara, S. Vizzini, B. Ealet, and B. Aufray, *Appl. Phys. Lett.* **97**, 223109 (2010).

¹⁰C. L. Lin, R. Arafune, K. Kawahara, N. Tsukahara, E. Minamitani, Y. Kim, N. Takagi, and M. Kawai, *Appl. Phys. Expr.* **5**, 045802 (2012).

¹¹B. J. Feng, Z. J. Ding, S. Meng, Y. G. Yao, X. Y. He, P. Cheng, L. Chen, and K. H. Wu, *Nano Lett.* **12**, 3507 (2012).

¹²A. Fleurence, R. Friedlein, T. Ozaki, H. Kawai, Y. Wang, and Y. Yamada-Takamura, *Phys. Rev. Lett.* **108**, 245501 (2012).

¹³A. Kara, H. Enriquez, A. P. Seitonen, L. C. Lew Van Voon, S. Vizzini, B. Aufray, and H. Oughaddou, *Surf. Sci. Rep.* **67**, 1 (2012).

¹⁴H. Sahin, S. Cahangirov, M. Topsakal, E. Bekaroglu, E. Akturk, R. T. Senger, and S. Ciraci, *Phys. Rev. B* **80**, 155453 (2009).

¹⁵L. Chen, C. C. Liu, B. J. Feng, X. Y. He, P. Cheng, Z. J. Ding, S. Meng, Y. G. Yao, and K. H. Wu, *Phys. Rev. Lett.* **109**, 056804 (2012).

¹⁶M. Ezawa, *New J. Phys.* **14**, 033003 (2012).

¹⁷M. Ezawa, *Phys. Rev. Lett.* **109**, 055502 (2012).

¹⁸Z. Y. Ni, Q. H. Liu, K. C. Tang, J. X. Zheng, J. Zhou, R. Qin, Z. X. Gao, D. P. Yu, and J. Lu, *Nano Lett.* **12**, 113 (2012).

¹⁹S. Cahangirov, M. Topsakal, E. Akturk, H. Sahin, and S. Ciraci, *Phys. Rev. Lett.* **102**, 236804 (2009).

²⁰C. C. Liu, H. Jiang, and Y. G. Yao, *Phys. Rev. B* **84**, 195430 (2011).

²¹X. T. An, Y. Y. Zhang, J. J. Liu, and S. S. Li, *New J. Phys.* **14**, 083039 (2012).

²²C. C. Liu, W. X. Feng, and Y. G. Yao, *Phys. Rev. Lett.* **107**, 076802 (2011).

²³N. D. Drummond, V. Zolyomi, and V. I. Fal'ko, *Phys. Rev. B* **85**, 075423 (2012).

²⁴S. Adachi, *Properties of Semiconductor Alloys, Group IV, III-V, and II-VI Semiconductors* (John Wiley & Sons, Chichester, UK, 2009).

²⁵M. L. Lee, E. A. Fitzgerald, M. T. Bulsara, M. T. Currie, and A. Lochtefeld, *J. Appl. Phys.* **97**, 011101 (2005).

²⁶H. Lin, R. S. Markiewicz, L. A. Wray, L. Fu, M. Z. Hasan, and A. Bansil, *Phys. Rev. Lett.* **105**, 036404 (2010).

²⁷W. Feng, D. Xiao, J. Ding, and Y. Yao, *Phys. Rev. Lett.* **106**, 016402 (2011).

²⁸B. A. Bernevig, T. L. Hughes, and S. C. Zhang, *Science* **314**, 17570 (2006).

²⁹L. Fu and C. L. Kane, *Phys. Rev. B* **76**, 045302 (2007).

³⁰J. C. Y. Teo, L. Fu, and C. L. Kane, *Phys. Rev. B* **78**, 045426 (2008).

³¹H.-J. Zhang, C.-X. Liu, X.-L. Qi, X.-Yu Deng, Xi Dai, S.-C. Zhang, and Z. Fang, *Phys. Rev. B* **80**, 085307 (2009).

³²P. Hohenberg and W. Kohn, *Phys. Rev.* **136**, B864 (1964).

³³W. Kohn and L. J. Sham, *Phys. Rev.* **140**, A1133 (1965).

³⁴The DFT code OpenMX is available at the website <http://www.openmx-square.org> in the constitution of the GNU General Public License; T. Ozaki, *Phys. Rev. B* **67**, 155108 (2003).

³⁵J. P. Perdew, K. Burke, and M. Ernzerhof, *Phys. Rev. Lett.* **77**, 3865 (1996).

³⁶G. Theurich and N. A. Hill, *Phys. Rev. B* **64**, 073106 (2001).

³⁷S. H. Wei, L. G. Ferreira, J. E. Bernard, and A. Zunger, *Phys. Rev. B* **42**, 9622 (1990).

³⁸P. Venezuela, G. M. Dalpian A. J. R. da Silva, and A. Fazzio, *Phys. Rev. B* **64**, 193202 (2001).

³⁹For weakly perturbed alloys, which is the case of the $\text{Si}_x\text{Ge}_{1-x}$ where the lattice mismatch is only 4%, it has been shown (Ref. 40) that it is possible to speak of an effective band structure for such a disordered system.

⁴⁰V. Popescu and A. Zunger, *Phys. Rev. Lett.* **104**, 236403 (2010).

⁴¹The bands shown in Fig. 3 are illustrative of particular SQS realizations for each x . However, for each SQS-generated configuration we have calculated its band structure, and they are all similar, as shown

in the Supplemental Material (Ref. 42). This collection of SQS band structures generates an energy dispersion for each k point (Ref. 40). The error bars in Fig. 3(a) were obtained from this dispersion at the K point.

⁴²See Supplemental Material at <http://link.aps.org/supplemental/10.1103/PhysRevB.88.201106> for the band structures of SQS realizations for $x = 26.5\%$, for the electronic properties of the ordered $\text{Si}_{0.5}\text{Ge}_{0.5}$ alloy and non-SQS disordered alloy, and for results for $3n \times 3n$ supercells.

⁴³When we refer to the gap in the text, we mean the distribution obtained from the different SQS-generated configurations (Refs. 40–42). It is important to stress that no averaging of these

results is performed, and that each one of the SQS configurations presents the same behavior.

⁴⁴A quadratic fit to $\Delta g(x) = ax - bx^2$ provides the coefficients $a = b = 14.0$ meV.

⁴⁵We have also performed calculations for $3n \times 3n$ supercells (6×6), where intervalley scattering becomes significant (Ref. 46). None of our conclusions have changed. This is in agreement with the findings of Jiang *et al.* (Ref. 46), where the authors show that disorder tends to weaken the effects of intervalley scattering whereas the effects of SOC are not affected.

⁴⁶H. Jiang, Z. Qiao, H. Liu, J. Shi, and Q. Niu, *Phys. Rev. Lett.* **109**, 116803 (2012).